Adapting to blur produced by ocular high-order aberrations

Lucie Sawides,
Instituto de Óptica, Consejo Superior de Investigaciones Científicas (CSIC), Madrid, Spain

Pablo de Gracia,
Instituto de Óptica, Consejo Superior de Investigaciones Científicas (CSIC), Madrid, Spain

Carlos Dorronsoro,
Instituto de Óptica, Consejo Superior de Investigaciones Científicas (CSIC), Madrid, Spain

Michael Webster, and
Department of Psychology, University of Nevada, Reno, NV, USA

Susana Marcos
Instituto de Óptica, Consejo Superior de Investigaciones Científicas (CSIC), Madrid, Spain

Abstract

The perceived focus of an image can be strongly biased by prior adaptation to a blurred or sharpened image. We examined whether these adaptation effects can occur for the natural patterns of retinal image blur produced by high-order aberrations (HOAs) in the optics of the eye. Focus judgments were measured for 4 subjects to estimate in a forced choice procedure (sharp/blurred) their neutral point after adaptation to different levels of blur produced by scaled increases or decreases in their HOAs. The optical blur was simulated by convolution of the PSFs from the 4 different HOA patterns, with Zernike coefficients (excluding tilt, defocus, and astigmatism) multiplied by a factor between 0 (diffraction limited) and 2 (double amount of natural blur). Observers viewed the images through an Adaptive Optics system that corrected their aberrations and made settings under neutral adaptation to a gray field or after adapting to 5 different blur levels. All subjects adapted to changes in the level of blur imposed by HOA regardless of which observer's HOA was used to generate the stimuli, with the perceived neutral point proportional to the amount of blur in the adapting image.

Keywords

Introduction

It is well known that the optics of the eye are not perfect (Artal, Guirao, Berrio, & Williams, 2001; Liang & Williams, 1997) and that the images projected on the retina are blurred by ocular aberrations that degrade image quality by attenuating contrast, reducing the range of spatial frequencies in the image, and introducing phase shifts. Moreover, the aberrations vary widely in magnitude and distribution in the population (Castejon-Mochon, Lopez-Gil, Benito, & Artal, 2002; Marcos & Burns, 2000; Porter, Guirao, Cox, & Williams, 2001;

Thibos, Hong, Bradley, & Cheng, 2002), and thus, individuals are each exposed to different long-term patterns of retinal blur. Recently, several studies have examined to what extent and in what ways the visual system can adjust to these variations in the optics and, in particular, have tried to assess the possible neural adaptations to optical blur.

Webster, Georgeson, and Webster (2002) found that brief periods of adaptation to blur can strongly affect the perception of image focus. Adapting to a sharpened image makes the physically focused image appear too blurred, whereas adapting to a blurred image makes a focused one appear sharper. Therefore, the subjective neutral point for image focus is shifted toward the sharpness or blur level of the adapting images. These aftereffects may reflect natural variants of the spatially selective adjustments studied extensively in the context of spatial frequency adaptation (Blakemore & Campbell, 1969; Blakemore & Sutton, 1969) and occur and can be selective for different types of images, for luminance or chromatic blur, spatial or temporal blur, and to different simulated depth planes (Battaglia, Jacobs, & Aslin, 2003; Bilson, Mizokami, & Webster, 2005; Webster et al., 2002; Webster, Mizokami, Svec, & Elliott, 2006), and thus, visual coding can readily adapt to many aspects of image blur.

An important question is whether adaptation also adjusts to the patterns of blur introduced by the eye's optics. A number of studies have, in fact, demonstrated adaptation aftereffects for images degraded by optical blur. For example, improvements in visual acuity occur following adaptation to optical defocus induced by wearing positive lenses (Mon-Williams, Tresilian, Strang, Kochhar, & Wann, 1998; Rosenfield, Hong, & George, 2004) or after a period of spectacle removal in myopes (Pesudovs & Brennan, 1993). Recently, we found that the adaptation can also be selective for the axis of astigmatism (Sawides, Gambra, Pascual, Dorronsoro, & Marcos, 2010). In that study, images simulating optical blur were generated by convolution with a combination of astigmatism and varying defocus in order to maintain constant total blur in the image, and subjects judged the orientation of the perceived blur. After adapting to horizontal astigmatism (so that blur in the images is predominantly along the horizontal axis), the perceived neutral point at which the blur appeared isotropic was shifted toward horizontally astigmatic images, with the opposite aftereffect following adaptation to vertical astigmatism.

The extent to which vision adapts to high-order aberrations is less certain, though the potential for adaptation has been suggested by several authors. Pesudovs (2005) suggested that adaptation to surgically induced HOA occurs in patients after LASIK surgery. Artal et al. (2004) showed that the stimuli seen through an individual's natural aberrations appear sharper than when seen through a rotated version of the same aberrations, suggesting that this may be a consequence of neural adaptation to the specific degradation produced by someone's HOA. Chen, Artal, Gutierrez, and Williams (2007) also found that subjective image quality was best when the observer's HOA was not fully corrected, though the implied adaptation was only a small fraction (~12%) of the effect predicted by complete adaptation.

Understanding the potential role of adaptation to optical aberrations is important because these aberrations can be and are routinely altered in a variety of ways. Certain treatments such as refractive surgery induce significant amounts of optical aberrations (Marcos, Barbero, Llorente, & Merayo-Lloves, 2001), while optical aids such as progressive spectacles produce significant amounts of astigmatism and field distortions (Villegas, Alcon, & Artal, 2006). Thus, how observers respond to these corrections may depend importantly on how they are able to neuronally adapt to these optical changes. Several ocular pathologies also alter the natural wave aberration of the eye (for example, keratoconus, which produces a progressive deformation of the cornea and an increase in the HOA of the eye; Barbero et

al., 2001). Sabesan and Yoon (2009) reported that keratoconic eyes do not achieve the visual benefit expected by the optical improvement and suggested that long-term adaptation to poor retinal image quality may limit the visual improvement immediately following correction. Conversely, they found better visual performance in real keratoconic eyes than normal eyes with a keratoconus wave aberration (simulated by Adaptive Optics), despite a similar optical degradation in both cases, which they attributed to adaptation to HOA in the keratoconic eyes (Sabesan & Yoon, 2010). Prior adaptation to the blur imposed by the optics was also attributed as the basis for discrepancies between predictions of optical performance under combined aberrations (astigmatism and coma) and visual performance in habitually uncorrected astigmats (de Gracia et al., 2010; de Gracia, Dorronsoro, Marin, Hernández, & Marcos, 2011). In addition, habitually uncorrected astigmats appeared more insensitive to the induction of astigmatism (with all low- and high-order aberrations corrected with adaptive optics) than non-astigmatic or normally corrected astigmatic subjects. In all previous examples, the fact that subjects with the same optical aberrations (achieved by manipulation of the wave aberration pattern with adaptive optics) exhibit very different relative visual performance to changes in the optics suggests that prior visual experience plays an important role in the visual response. Alternatively, the ultimate goal of refractive correction is the elimination of HOA of the eye. Debate is ongoing whether patients adapt to their new pattern of optical aberrations so that vision is less compromised than the optical degradation of their retinal image quality would suggest, if aberrations have been induced, or conversely, whether they can take advantage of an improved image quality if aberrations have been corrected. For example, Marcos, Sawides, Gambra, and Dorronsoro (2008) and Rossi and Roorda (2010) showed, in most cases, an immediate improvement of visual acuity upon correction of high-order aberrations that showed a minimal effect of short-term adaptation or perceptual learning. However, as noted by the authors, their study did not assess the potential effects of adaptation on subjective image quality or on visual acuity or sensitivity to natural images. Thus, the potential impact of adaptation on refractive corrections remains unknown. In addition, we found in a subjective image sharpness assessment experiment that observers chose as "the sharpest image" 84% on average of the images seen through a full correction of their HOA (Sawides, Gambra et al., 2010). The correction of HOA produces, therefore, a clear increase of the subjective impression of sharpness. However, the question remains open whether the sharpest image actually appears "too sharp" to the subject because they are adapted to compensate for their aberrations. In these prior studies, adaptation to HOA was only implicitly tested by asking how perceived image quality or acuity changed with a change in the aberration pattern. In the current study, we instead directly tested whether subjects can adapt to changes in the magnitude of HOA, by measuring the aftereffects of exposure to different levels of HOA on subjective image focus. We used a similar paradigm to that used by Webster et al. (2002) to study aftereffects following adaptation to blur or sharpened images. However, rather than artificial symmetric blur (introduced by filtering the image), we tested for potential aftereffects after adaptation to various levels of blur produced by actual HOA centered around the actual magnitudes of blur that the observers were normally exposed to (simulated in the image while subjects viewed the stimuli with their native HOA corrected with AO). Subjects were exposed to their own aberrations as well as other subject's aberrations. We also explored the dependence of the effect on the amount of blur in the adapting image, as well as the transfer of the effect across different adapting and test images.

Methods

Adaptive optics setup

The experiments were performed using a custom-built Adaptive Optics system provided with a psychophysical channel, developed at the Visual Optics and Biophotonics Laboratory

(Institute of Optics, CSIC). The primary components of the system were a Hartmann–Shack wavefront sensor (HASO 32 OEM, Imagine Eyes, France) and an electromagnetic deformable mirror (MIRAO, Imagine Eyes, France). A motorized Badal system compensated for the subject's spherical error. Two psychophysical displays were used for stimulus presentation. The first channel, composed of a 12 mm × 9 mm SVGA OLED minidisplay (LiteEye 400), was used for fixation during the measurement and correction of the subject's aberration. The second channel, composed of a 12 × 16 inch Mitsubishi Monitor and controlled by the ViSaGe psychophysical platform (Cambridge Research System, UK), was used to present the natural grayscale images of the experiment. The system was controlled using custom routines written in Visual C++ (to control the AO loop and the Badal system) and Matlab (to control the ViSaGe). Specific details of the AO system are reported in previous articles (de Gracia et al., 2010, 2011; Marcos et al., 2008; Sawides, Gambra et al., 2010).

Correction of ocular aberrations

The aberrations were corrected in a closed loop at 13 Hz in 15 iterations, with the state of the deformable mirror (voltage applied to each actuator) that best corrected astigmatism and HOA saved and applied. The correction was checked before and after each psychophysical setting and deemed satisfactory when the correction was higher than 70% or the residual wavefront error is less than 0.15 μm RMS (excluding tilts and defocus). On average, RMS error correction was 78 ± 8%. All measurements were performed for best subjective defocus, with corrected astigmatism and AO obtained with a Badal system.

Subjects

Four of the authors, aged 27 to 39 years, were tested in the experiment, with HOA RMS ranging from 0.18 to 0.39 μm (5-mm pupils). All protocols met the tenets of the Declaration of Helsinki.

Stimuli

The original images were acquired using a digital camera (Canon PowerShot) with a resolution of 4 megapixels. The original image was converted to grayscale and a resolution of 480 by 480 pixels, and then blurred by convolution with the PSF estimated from each subject's natural aberrations. Aberrations of the subject were measured using the AO setup and fitted to 7th-order Zernike polynomials. Tilts, astigmatism, and defocus were set to zero, except for a control experiment where defocus was optimized to maximize Strehl. Standard Fourier optics techniques (Goodman, 1996), including the Fast Fourier Transform programmed in Matlab, were used to calculate the corresponding Point Spread Function (PSF). The PSF was scaled to match the pixel size of the face image in 1.98° window. All computations were performed for 5-mm pupils. The Stiles–Crawford effect was not considered, as for typical ρ values ($\rho < 0.1$; Marcos & Burns, 2009) its effect was negligible for the purposes of our study. A double diffraction when viewing the convolved image through a diffraction-limited 5-mm pupil (convolution + artificial pupil aperture) was not corrected by means of inverse filtering, as it was considered negligible. Simulations conducted to assess the impact of these two factors revealed that the effect on the final contrast of convolved E targets with similar levels of blur to those used on the experiment was less than 10% with respect to the contrast obtained without including these two factors. The use of convolved images to represent the retinal image quality has been largely used in visual optics (Applegate, Marsack, Ramos, & Sarver, 2003; Burton & Haig, 1984; Peli & Lang, 2001), although there are recent reports showing systematic differences in the visual acuity measured using simulated versus real aberrated targets (de Gracia, Dorronsoro, Sawides, Gambra, & Marcos, 2009; Ohlendorf, Tabernero, & Schaeffel, 2011). We performed calibrations and control experiments using a CCD camera as an artificial retina to

ensure the correct representation (in scale and contrast) of the projected images, within the experimental error of the CCD image acquisition. In any case, as the measurements represent relative shifts, potential discrepancies in both the adapting and test images should not affect the results.

Different sets of images were generated for each subject's HOA. For each HOA pattern, a sequence of images was created by multiplying each Zernike coefficient by a factor (F) between 0 and 2 in 0.05 steps. Each set of testing images, thus, contained 41 different images ranging from diffraction-limited to double the amount of natural blur. For $F = 1$, the simulated image represented the natural degradation imposed by the HOA. For adapting images, we used 5 different levels of blur ($F = 1$, the native aberration; $F = 0$ and $F = 0.5$ for adaptation to sharper images; and $F = 1.5$ and $F = 1.9$ for adaptation to more blurred images). Multiplying the Zernike coefficients by these factors modified the amount of blur while preserving the relative shape of the PSF. Images were presented at optical infinity for the observers and subtended 1.98 deg. Figure 1 illustrates the image simulation procedure, for different scaling factors.

Experimental protocols

Measurements were done under natural viewing conditions in a darkened room. An artificial pupil in a pupil conjugate plane guaranteed that the measurements were performed under a constant pupil size of around 5-mm pupil diameter. Each experiment was conducted in a single session for each subject, lasting approximately 4 h.

The subject's pupil was aligned to the system using a bite bar and the pupil was centered and focused. The subject was then asked to adjust the best subjective focus, by controlling the Badal system with a keyboard while he/she looked at a high-contrast Maltese cross on the minidisplay.

Natural aberrations (with the exception of tilts and defocus) were measured and corrected in a closed-loop adaptive-optics operation. The subject was then asked again to adjust the Badal system position to provide the best subjective focus for the AO-corrected condition. The state of the mirror that achieved this correction was saved and applied during the measurements. Psychophysical measurements were performed under static corrections of aberrations. However, the natural pupil was continuously monitored to ensure centering, before and during the test, and as noted, the wave aberration was measured before and after each test (i.e., every 5 min) to ensure appropriate AO correction (with a new closed-loop correction applied if needed).

Psychophysical paradigm and sequence

All experiments were performed under full AO-corrected aberrations and best spherical refraction error correction. The psychophysical paradigm consisted of a two-alternative forced-choice procedure (2AFC), where the subject had to respond whether the image was sharp or blurred. Test levels were chosen based on a QUEST algorithm in order to find the best perceived focus point for a given condition of adaptation.

Each subject performed the test for 6 different conditions: after neutral adaptation (to a gray screen) and after adaptation to 5 different levels of blur: 2 levels of sharper images ($F = 0$; $F = 0.5$), a natural aberration level ($F = 1$), and 2 levels that were more blurred ($F = 1.5$; $F = 1.9$). Each subject was tested using the sequence of images generated with their own aberrations and with those generated using the other three subjects' aberrations.

In the first experiment, the test and adapting images were the same (an image of author LS's face). In the second experiment, observers again adapted to the image of LS but were tested

on an image from a different face (author SM), in order to assess the transfer of the adaptation effect across images. A total of 24 conditions were tested in each experiment, as illustrated in Figure 2. The same sequence was tested on all 4 subjects (except S1, who did not perform the test with the S4 wavefront (WF) sequences, because of the larger natural amount of HOA for S1, which doubles the amount of natural HOA of S4).

A control experiment was performed on one observer (S4), similar to Experiment 1, where the subject adapted to his own aberrations and tested with 4 sequences of images generated with each subjects' aberrations and, alternatively, adapted to the other 3 subjects' aberrations and was then tested with the image sequence generated with his own aberrations. This experiment was designed to examine whether the perceived focus point was specific to the specific degradation produced by a certain pattern of aberrations, or rather to the overall level of blur, regardless the aberration pattern. In order to increase the range and resolution of the image sequence, the HOAs (for S4) were multiplied by a factor between 0 and 4 (instead of 0 and 2) and the generation of images was refined by setting the defocus to optimize the optical quality of the images (instead of setting it to 0).

In all cases, the sequence of the psychophysical experiment consisted of an initial 1-min adaptation to the adapting image after which a test image was presented for 1 s to the subject who had to respond if the image was sharp or blurred. The adapting image was reshown for 3 s in between each test presentation until the threshold was determined. Neutral settings (adaptation to gray field) were repeated three times in each subject. The standard deviation of those measurements was used as an estimate of the typical measurement error. The other conditions were only performed once.

Data analysis

Aberrations—Wave aberrations were fitted by 7th-order Zernike polynomial expansions. Optical quality was evaluated in terms of RMS wavefront error (excluding tilts and defocus).

Best perceived focus point—The perceived focus point usually converges, in the 2AFC procedure, to the final value in less than 35 trials or 16 reversals. At the end of each setting, the perceived focus point is checked to be stable over the last 8 reversals and the perceived focus point was obtained as the average of these 8 last reversals of the 2AFCP.

The results were analyzed in terms of the perceived focus point selected after adaptation to different levels of blur. Data were analyzed as a function of factor *F* (relative blur) and RMS of the wave aberration used to degrade the image (absolute blur).

Results

Best corrected ocular aberrations

Figure 3 shows RMS wavefront error and wave aberrations (excluding tilts and defocus) for all subjects of the study before and after AO correction of aberrations. Data are for 5-mm pupil diameters. Subject S1 performed the measurements wearing her soft contact lenses. On average, RMS (excluding tilts and defocus) decreased from 0.539 ± 0.311 to 0.105 ± 0.046 μm, with an average correction of $78 \pm 8\%$.

Adaptation to blur produced by HOA

Figure 4 shows the perceived neutral focus point of each subject after adaptation to images generated using each subject's own HOA, for the 6 levels of blur (gray field, sharpened, natural HOA, and blurred images). Again, for this experiment, a single face image was used

for both adaptation and test. The blur level is represented in terms of factor F, i.e., the amount of blur relative to the natural aberration of each subject. After adapting to a sharper image, the subjective neutral focus point shifts to sharper levels and after adapting to a blurred image, the subjective neutral focus point shifts to more blurred levels. Typical errors (standard deviation of factor F) were 0.045 on average across subjects—from repeated measurements on the gray adaptation condition/test with their own HOA/LS face—which corresponded to less than 7% error.

Figure 5 shows subjective neutral points for two of the 4 subjects, after adaptation to images generated using his/her own HOA and other subjects' HOA. The results were similar for all subjects. The shift (compared to the natural condition) in the subjective neutral focus occurs in all cases, regardless of the wave aberration pattern used to generate the image. Typical errors (standard deviation of factor F) were 0.080 on average, which corresponded to around 12% error.

Adaptation as a function of the amount of blur in the adapting image

The data set of Experiment 1 allows us to assess whether the size of the aftereffect is proportional to the amount of blur in the adapting image, both within the images generated by scaling of a given wave aberration pattern and within the range of blur produced by natural aberrations. Figure 6 shows the perceived neutral focus point in terms of absolute RMS blur. Each point is the average setting across subjects. When adapting to images generated with low amounts of HOA, the perceived focus point is lower than when adapting to images generated with higher amounts of HOA, and this occurs at all adapting conditions. Therefore, the neutral point is proportional to the amount of adapting blur. Saturation occurs at the more blurred level in each sequence for all subjects. At all levels of blur in the adapting image, there is a highly significant correlation between the perceived neutral focus point and the blur of the adapting image (in terms of RMS). Adaptation to a sharp image ($F = 0$) shifted the perceived focus point toward sharper levels by -0.14 ± 0.04 μm RMS on average, while adapting to a blurred image ($F = 1.5$) shifted the neutral focus point to more blurred levels by 0.07 ± 0.03 μm on average. The magnitude of the effect can be assessed by referring to the images in Figure 2, where the image degradation for all subjects and different F factors is illustrated.

Figure 7 shows the results of the control experiment for one subject (S4), adapting to the other subjects' aberrations (and using the test image sequence generated with his own aberrations) or adapting to his own aberrations (and using test image sequences generated with the aberrations of the remaining subjects). As expected from Experiment 1, when adapting to images with different amounts of blur (corresponding to the natural aberrations of the different subjects), the perceived focus point shifts proportionally to the amount of blur in the adapting image (note that this subject had the lowest RMS aberrations and, thus, was adapted to higher levels of blur when exposed to the aberrations of the other subjects). Interestingly, for a similar adapting image (his own aberrations), the perceived focus point is rather constant, regardless of the specific pattern of degradation of the test image sequence.

Adaptation transfer across images

In the preceding experiments, the test and adapt stimuli were drawn from the same image. In the next experiment, we again adapted to the same image (of author LS) but then tested aftereffects by varying blur level in a different image (of author SM), again testing all subjects and the 6 conditions of adaptation. Typical errors (standard deviation of factor F) were 0.028 on average across subjects, which corresponded to less than 4% error. The results are plotted in Figure 8. As in the first experiment, the subjective focus point shifts to sharper levels after adapting to a sharpened image and to more blurred levels after adapting

to a blurred image. The results, therefore, show that the adaptation effect transfers across different (albeit similar) images, consistent with the transfer found for artificial blur (Webster et al., 2002).

We again analyzed the settings as a function of absolute RMS blur (as in Figure 6). Figure 9 revealed significant correlations and similar regressions between blur in the adapting image and blur level of the perceived focus point. The effects are similar to those found in the previous experiment (same adapting and test images) except for the more blurred level, where we do not see the saturation effect when using different adapting and test images.

Finally, Figure 10 compares the perceived focus point obtained using the same or different images for testing and adapting, averaged across subjects. The results from both experiments are strongly correlated (p-value < 0.001, $R = 0.89$), suggesting that there was nearly complete transfer of the blur adaptation across the two different face images.

Discussion

Previous studies have shown that the perception of image blur can be strongly affected by adaptation to images that have been artificially blurred or sharpened (Webster et al., 2002) and that these aftereffects can also occur for the natural patterns of blur produced by low-order aberrations of the eye's optics (Sawides, Marcos et al., 2010). The present results extend these findings by showing that adaptation also occurs for the patterns of natural blur produced by the high-order aberrations of the eyes. The use of an Adaptive Optics system has allowed us to pre-compensate the natural aberrations of the eyes and, therefore, expose all subjects to the same amounts and patterns of blur, ensuring that any difference across subjects will arise from their own neural processing or prior neural adaptation. As the measurements represent relative shifts, potential discrepancies in both the adapting and test images, the use of convolved images to represent the retinal image quality should not affect the results. Furthermore, the fact that the blur level of the perceived focus shift is similar under natural and gray adaptation supports the appropriate representation of blur in the simulated images.

For all subjects, there was a systematic shift of the perceived neutral focus after exposure to more blur when adapting to an image blurred by a scaled increase in the natural HOA ($F > 1$) and to less blur when adapting to an image sharpened by a scaled decrease in the HOA ($F < 1$). Interestingly, these adaptation effects occurred not only when subjects adapted to scaled versions of their own HOA but also to the aberration pattern from other subjects. Moreover, we found that the shift of the neutral point after adaptation is proportional to the absolute amount of blur of the adapting image, regardless of whether the blur is produced by increasing the size of the PSF or by natural aberrations found in different eyes. The results, thus, strongly suggest that changes in the magnitude of HOA—within the natural range characteristic of actual eyes—can strongly influence the state of blur adaptation in the visual system. (Notably, the perceived neutral point found after adapting to the natural HOA pattern was slightly lower than expected, (i.e., the factor F of the perceived neutral point is <1), which may be attributed to some residual defocus arising in the simulated degradation from setting defocus term to 0. A control experiment where the defocus term was set to optimize the optical quality of the simulated image produced an excellent correspondence between the blur level of the perceived neutral point and the amount of natural aberrations of a given eye.)

However, it remains to be tested whether the adaptation is selective for different types of combinations of HOA, in the way it has been shown to be selective for differences in low-order aberrations and astigmatism in particular (Sawides, Marcos et al., 2010). The

experiment in which the observer adapted to their own aberrations and then adjusted the perceived focus by varying the magnitude of a different observer's HOA or vice versa suggested that the adaptation effect is largely driven by the overall level of blur contained in the adapting images more than by the specific shape of the HOA pattern. This suggests that the aftereffects we measured depended largely on the global level of blur rather than local features associated with the asymmetric blur arising from particular HOA. However, our test stimuli did not, in fact, vary in ways that might capture aberration-selective aftereffects. To directly test for this pattern selectivity would require varying the stimulus between two different aberration patterns (e.g., with the same RMS blur level) and then assessing whether adaptation to one of the patterns biased the perceived pattern of blur toward the unadapted pattern (in the same way that adaptation to vertical astigmatism biases an isotropic pattern toward horizontally oriented blur; Sawides, Marcos et al., 2010). The results of Artal et al. (2004) showing variations in perceived image quality for rotated versions of the same HOA are consistent with an influence of the blur pattern on the adaptation.

Our present results also leave open the question of how selective the aftereffects are for changes in other properties of the images. We showed that there is almost complete transfer of the adaptation across different images of faces, suggesting that the adaptation is at least partly adjusting to the attribute of blur independently of the specific image structure. However, it remains to be seen to what extent this transfer occurs for more dissimilar images.

The fact that eyes can adapt to blur imposed by high-order aberrations has important practical implications, as the aberrations of the eye are routinely altered either in the course of pathology or aging, or artificially by ophthalmic, contact, or intraocular lenses and corneal refractive surgery procedures.

Although our data relate to changes in the perception of normal blur and are not necessarily extrapolated to changes (or improvement) in visual function following adaptation, they suggest that patients can adapt perceptually to a change in the amount of these aberrations. In this sense, the perceptual changes in focus judgments following adaptation may be associated with the reported improvement of VA over time in patients following refractive surgery (which induced significant amount of aberrations; Pesudovs, 2005), the relatively better VA in keratoconic eyes compared to normal eyes with similar induced aberrations (Sabesan & Yoon, 2010), or habitually non-corrected astigmats compared to normal eyes with induced astigmatism (de Gracia et al., 2011).

Conclusions

Adaptation occurs to changes in the natural levels of blur produced by high-order aberrations. The perceived best focus is proportional to the amount of blur, produced by both changing the size of the blur (preserving its shape) and the amount and pattern of aberrations across different eyes. The results also suggest that the adaptation aftereffects depended largely on the global level of blur rather than local features associated with the asymmetric blur arising from particular HOA. Moreover, adaptation to the fully corrected HOA produced aftereffects equivalent to a sharpened adapter, while adaptation to a more blurred image induce an aftereffect that was shifted toward the more blurred level of their natural HOA. These results demonstrate that the eye can adapt to the levels of blur produced by HOA and suggest that adaptation may be an important factor in understanding the perceptual changes that occur when HOA are altered by pathology or surgery.

Acknowledgments

References

Applegate RA, Marsack JD, Ramos R, Sarver EJ. Interaction between aberrations to improve or reduce visual performance. Journal of Cataract & Refractive Surgery. 2003; 29:1487–1495. [PubMed: 12954294]

Artal, P.; Chen, L.; Fernandez, EJ.; Singer, B.; Manzanera, S.; Williams, DR. Neural compensation for the eye's optical aberrations; Journal of Vision. 2004. p. 4p. 281-287.http://www.journalofvision.org/content/4/4/4

Artal, P.; Guirao, A.; Berrio, E.; Williams, DR. Compensation of corneal aberrations by the internal optics in the human eye; Journal of Vision. 2001. p. 1p. 1-8.http://www.journalofvision.org/content/1/1/1

Barbero S, Marcos S, Martín R, Llorente L, Moreno-Barriuso E, Merayo-Lloves JM. Validating the calculation of corneal aberrations from corneal topography: A test on keratoconus and aphakic eyes. Investigative Ophthalmology & Visual Science. 2001; 42:894.

Battaglia PW, Jacobs RA, Aslin RN. Depth-dependent blur adaptation. Vision Research. 2003; 44:113–117. [PubMed: 14637361]

Bilson AC, Mizokami Y, Webster MA. Visual adjustments to temporal blur. Journal of the Optical Society of America A, Optics, Image Science, and Vision. 2005; 22:2281–2288.

Blakemore C, Campbell FW. On the existence of neurones in the human visual system selectively sensitive to the orientation and size of retinal images. The Journal of Physiology. 1969; 203:237–260. [PubMed: 5821879]

Blakemore C, Sutton P. Size adaptation: A new aftereffect. Science. 1969; 166:245–247. [PubMed: 5809598]

Burton GJ, Haig ND. Effects of the Seidel aberrations on visual target discrimination. Journal of the Optical Society of America A. 1984; 1:373–385.

Castejon-Mochon JF, Lopez-Gil N, Benito A, Artal P. Ocular wave-front aberration statistics in a normal young population. Vision Research. 2002; 42:1611–1617. [PubMed: 12079789]

Chen, L.; Artal, P.; Gutierrez, D.; Williams, DR. Neural compensation for the best aberration correction; Journal of Vision. 2007. p. 9p. 1-9.http://www.journalofvision.org/content/7/10/9

de Gracia P, Dorronsoro C, Gambra E, Marin G, Hernández M, Marcos S. Combining coma with astigmatism can improve retinal image over astigmatism alone. Vision Research. 2010; 50:2008–2014. [PubMed: 20659497]

de Gracia, P.; Dorronsoro, C.; Marin, G.; Hernández, M.; Marcos, S. Visual acuity under combined astigmatism and coma: Optical and neural adaptation effects; Journal of Vision. 2011. p. 5p. 1-11.http://www.journalofvision.org/content/11/2/5

de Gracia, P.; Dorronsoro, C.; Sawides, L.; Gambra, E.; Marcos, S. Adaptive optics: Methods, analysis and applications, OSA Technical Digest [CD], Paper JWB4. Optical Society of America; 2009. Experimental test of simulated retinal images using adaptive optics.

Goodman, JW. Introduction to Fourier optics. 2. New York: McGraw-Hill; 1996.

Liang J, Williams DR. Aberrations and retinal image quality of the normal human eye. Journal of the Optical Society of America A. 1997; 14:2873–2883.

Marcos S, Barbero S, Llorente L, Merayo-Lloves J. Optical response to LASIK surgery for myopia from total and corneal aberration measurements. Investigative Ophthalmology & Visual Science. 2001; 42:3349–3356. [PubMed: 11726644]

Marcos S, Burns SA. On the symmetry between eyes of wavefront aberration and cone directionality. Vision Research. 2000; 40:2437–2447. [PubMed: 10915884]

Marcos S, Burns SA. Cone directionality from laser ray tracing in normal and LASIK patients. Journal of Modern Optics. 2009; 56:2181–2188.

Marcos, S.; Sawides, L.; Gambra, E.; Dorronsoro, C. Influence of adaptive-optics ocular aberration correction on visual acuity at different luminances and contrast polarities; Journal of Vision. 2008. p. 1p. 1-12.http://www.journalofvision.org/content/8/13/1

Mon-Williams M, Tresilian JR, Strang NC, Kochhar P, Wann JP. Improving vision: Neural compensation for optical defocus. Proceedings of the Royal Society B: Biological Sciences. 1998; 265:71–77.

Ohlendorf A, Tabernero J, Schaeffel F. Visual Acuity with simulated and real astigmatic defocus. Optometry & Vision Science. 2011; 88:1–8. [PubMed: 21191284]

Peli E, Lang A. Appearance of images through a multifocal intraocular lens. Journal of the Optical Society of America A, Optics, Image Science, and Vision. 2001; 18:302–309.

Pesudovs K. Involvement of neural adaptation in the recovery of vision after laser refractive surgery. Journal of Refractive Surgery. 2005; 21:144–147. [PubMed: 15796218]

Pesudovs K, Brennan NA. Decreased uncorrected vision after a period of distance fixation with spectacle wear. Optometry & Vision Science. 1993; 70:528–531. [PubMed: 8355963]

Porter J, Guirao A, Cox IG, Williams DR. Monochromatic aberrations of the human eye in a large population. Journal of the Optical Society of America A, Optics, Image Science, and Vision. 2001; 18:1793–1803.

Rosenfield M, Hong SE, George S. Blur adaptation in myopes. Optometry & Vision Science. 2004; 81:657–662. [PubMed: 15365384]

Rossi, EA.; Roorda, A. Is visual resolution after adaptive optics correction susceptible to perceptual learning?; Journal of Vision. 2010. p. 11p. 1-14.http://www.journalofvision.org/content/10/12/11

Sabesan, R.; Yoon, G. Visual performance after correcting higher order aberrations in keratoconic eyes; Journal of Vision. 2009. p. 6p. 1-10.http://www.journalofvision.org/content/9/5/6

Sabesan R, Yoon G. Neural compensation for long-term asymmetric optical blur to improve visual performance in keratoconic eyes. Investigative Ophthalmology & Visual Science. 2010; 51:3835–3839. [PubMed: 20130284]

Sawides, L.; Gambra, E.; Pascual, D.; Dorronsoro, C.; Marcos, S. Visual performance with real-life tasks under adaptive-optics ocular aberration correction; Journal of Vision. 2010. p. 19p. 1-12.http://www.journalofvision.org/content/10/5/19

Sawides, L.; Marcos, S.; Ravikumar, S.; Thibos, L.; Bradley, A.; Webster, MA. Adaptation to astigmatic blur; Journal of Vision. 2010. p. 22p. 1-15.http://www.journalofvision.org/content/10/12/22

Thibos LN, Hong X, Bradley A, Cheng X. Statistical variation of aberration structure and image quality in a normal population of healthy eyes. Journal of the Optical Society of America A, Optics, Image Science, and Vision. 2002; 19:2329–2348.

Villegas, EA.; Alcon, E.; Artal, P. Investigative Ophthalmology & Visual Science. Vol. 47. 2006. The effect of correcting small astigmatisms on visual acuity; p. E-Abstract, 1173

Webster MA, Georgeson MA, Webster SM. Neural adjustments to image blur. Nature Neuroscience. 2002; 5:839–840.

Webster MA, Mizokami Y, Svec LA, Elliott SL. Neural adjustments to chromatic blur. Spatial Vision. 2006; 19:111–132. [PubMed: 16862835]
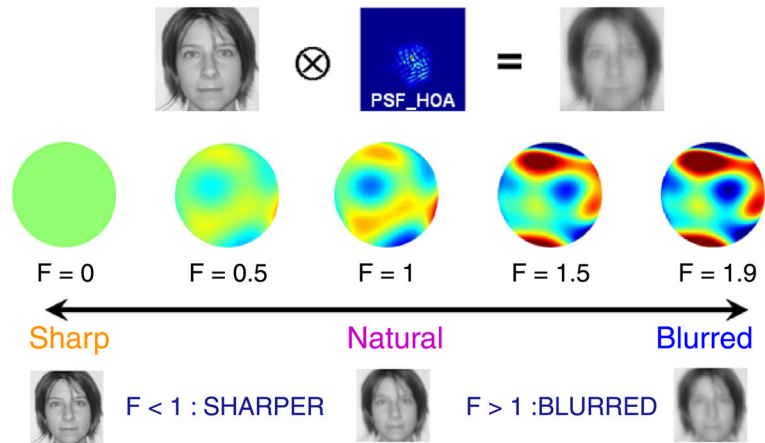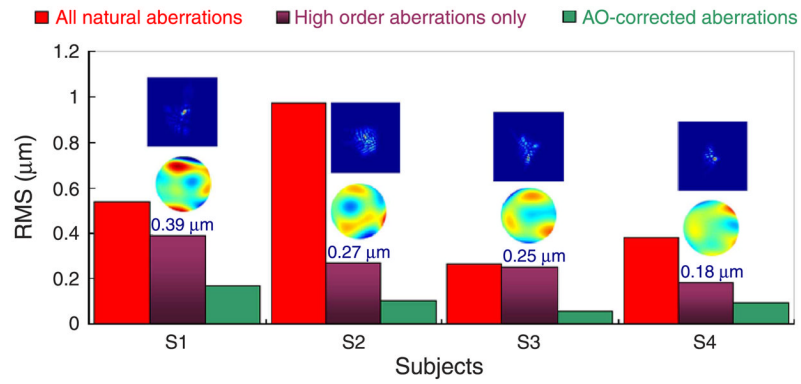
Figure 1.
Illustration of the procedure to generate the sequences of testing and adapting images. The images are degraded by convolution with the PSF corresponding to an observer's natural wave aberrations. The sequence of images was achieved by scaling the wave aberration by different multiplicative factors *F* (see text for details).
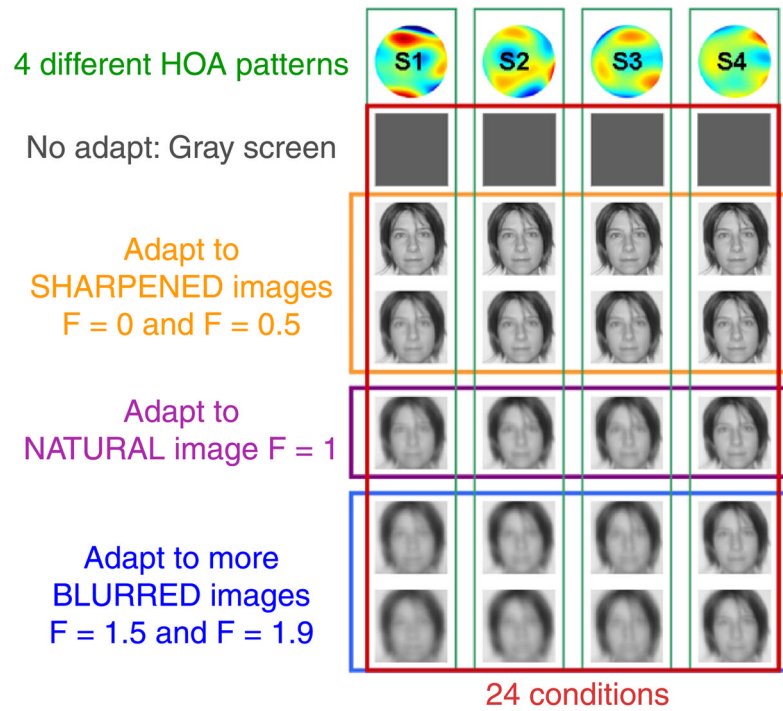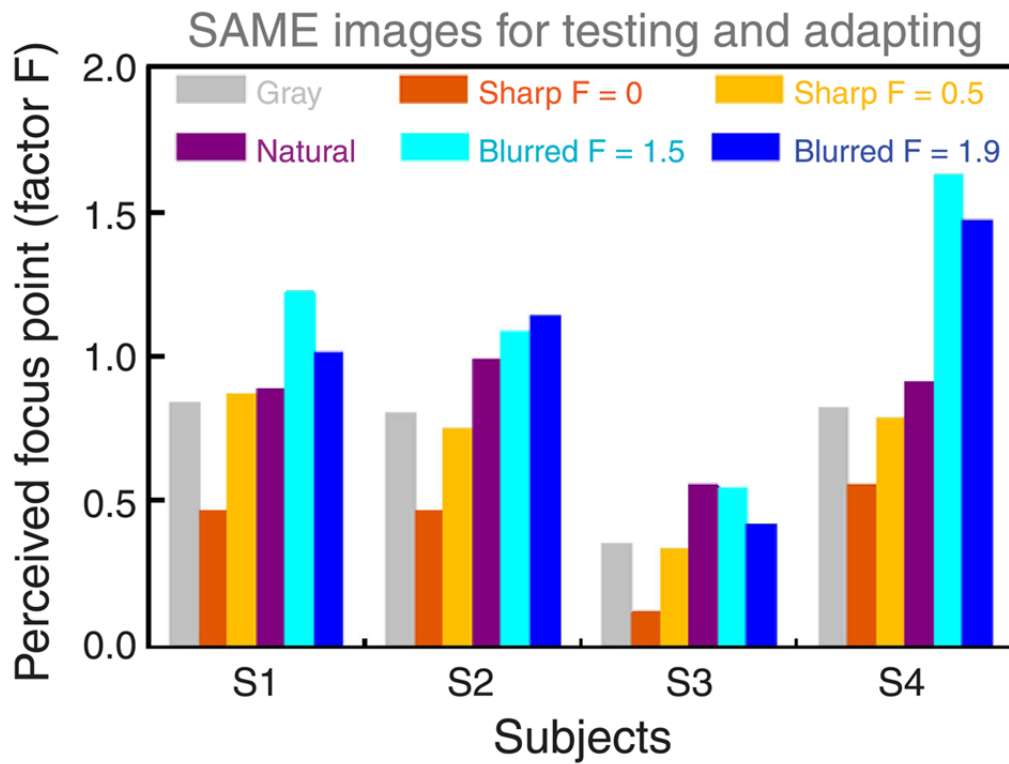
Figure 2.
Wave aberration patterns (top row) and the 24 adapting conditions, tested in both experiments.

Figure 3.
RMS wavefront error (excluding tilts and defocus; red), RMS for HOA (excluding tilts, defocus, and astigmatism; purple), and AO correction (correction of defocus, astigmatism, and HOA; green). The corresponding RMS wave aberrations and PSF for the HOA of each subject are depicted above the purple bars. Measurements were for 5-mm-pupil diameters.
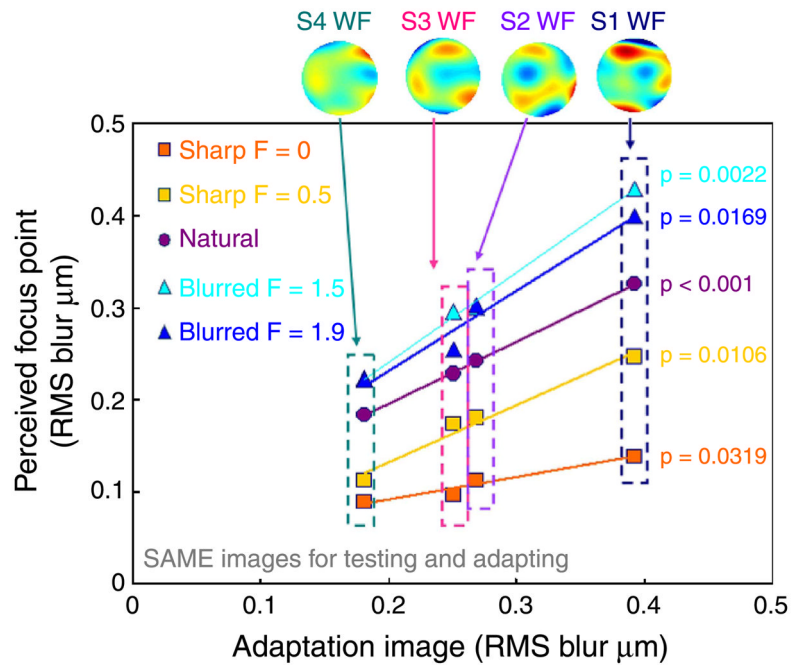
Figure 4.
Perceived focus point for each subject when adapting to a gray field and to images degraded using his/her own wave aberration (and scaled versions of it). The experiment was performed with the same images (LS) for testing and adapting.
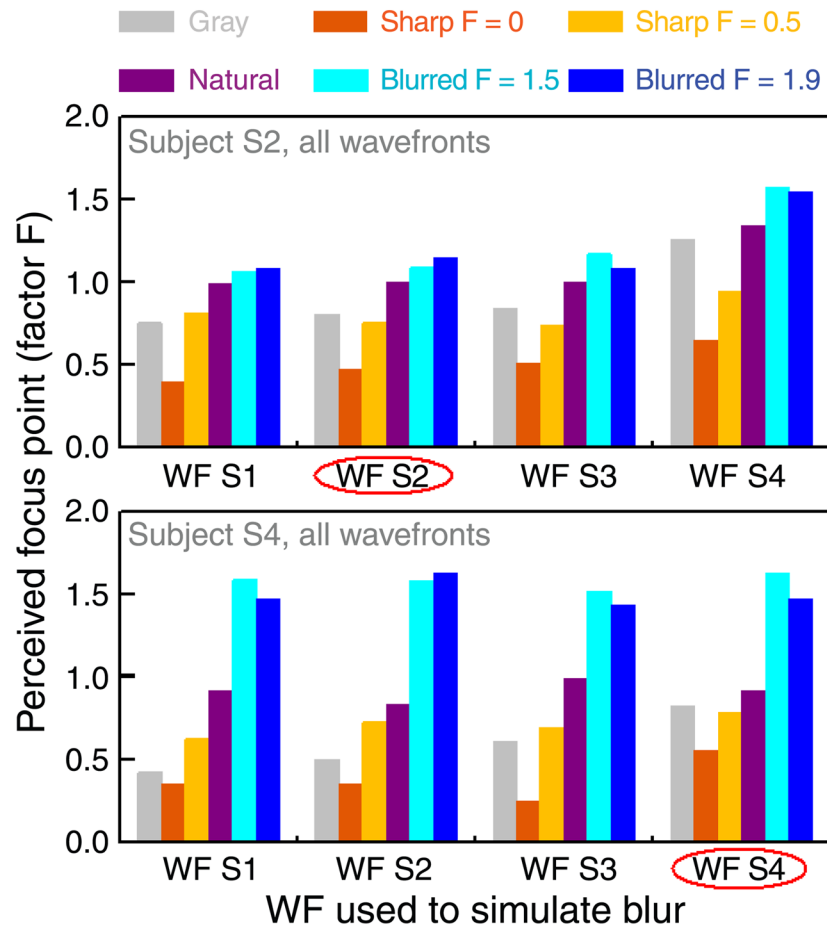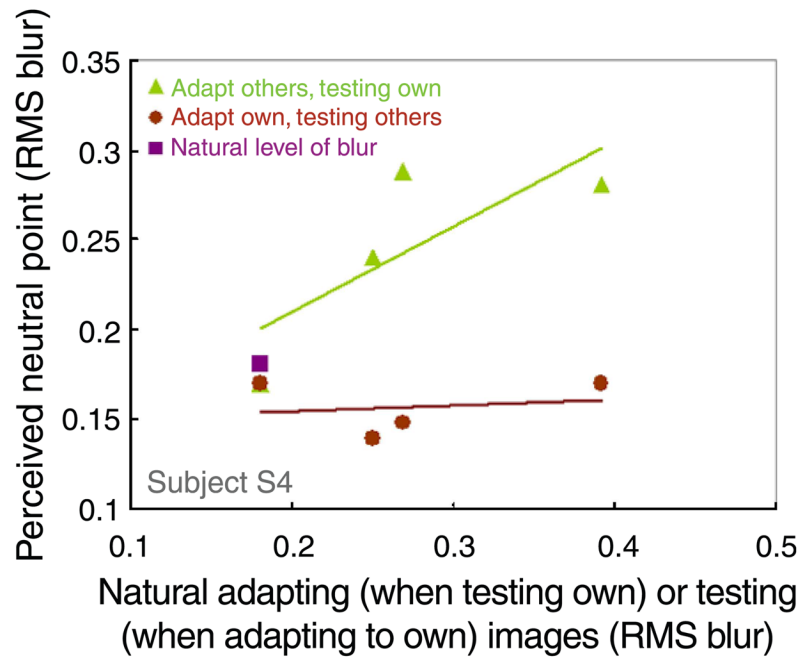
Figure 5.
Perceived focus point for all conditions of adaptation. The case where adapting images were generated using the subject's own aberration is indicated by a red ellipse. The different colors represent the focus shift for different amounts of blur (*F*) relative to the natural aberrations. Results are for subjects S2 (upper panel) and S4 (lower panel).
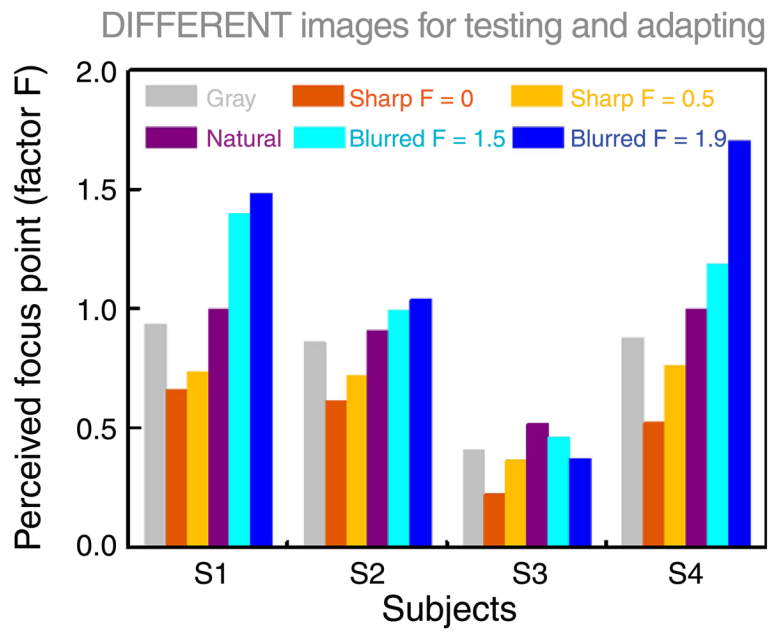
Figure 6.
Perceived focus point in terms of RMS (μm) when adapting to images blurred within the range of normal amounts of HOA, on average across subjects (same images for testing and adapting).
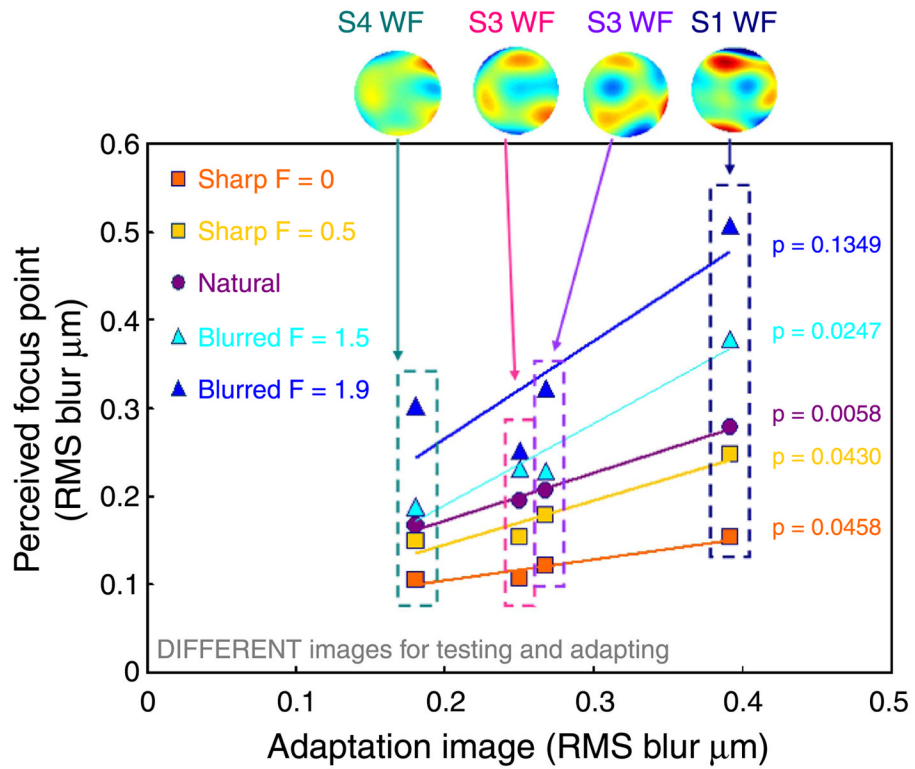
Figure 7.
Perceived focus point in terms of RMS (μm) as a function of the blur of the adapting image (green triangles) or as a function of the aberrations of the central image test ($F = 1$) of the sequence of test images (brown circles). The purple square represents the natural RMS of the subject. In the first case (green triangles), the test sequence was generated from the subject's own aberrations and the subject adapted to each subject's aberrations. In the second case (brown circles), the test sequences were generated from the other subjects' aberrations and the subject adapted to their own natural aberrations. Data are for subject S4 (same images, LS, for testing and adapting).
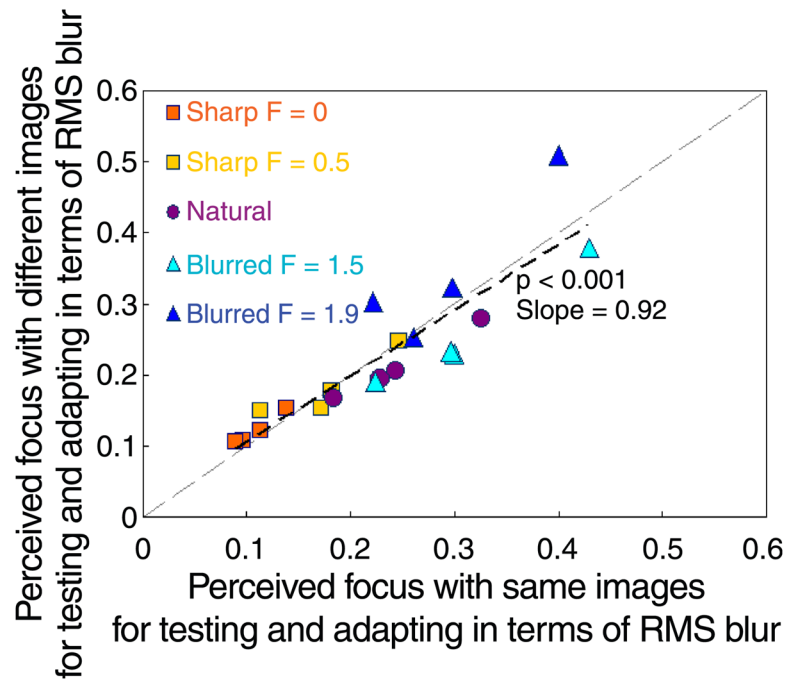
Figure 8.
Perceived focus point for each subject when adapting to a gray field and to images degraded using his/her own wave aberration and scaled versions of it (different images for testing and adapting).

Figure 9.
Perceived focus point in terms of RMS (μm) when adapting to images blurred within the range of normal amount of HOA, on average across subjects (different images for testing and adapting).

Figure 10.
Perceived focus point for the same versus different adapt and test images. Data are averaged across subjects.